Hydrothermal Synthesis of Microporous Tin Sulfides Studied by Real-Time in Situ Energy-Dispersive X-ray Diffraction

R. J. Francis, S. J. Price, J. S. O. Evans, S. O'Brien, and D. O'Hare*

Inorganic Chemistry Laboratory, University of Oxford, South Parks Road, Oxford, UK OX1 3QR

S. M. Clark

Daresbury Laboratory, Daresbury, Warrington, UK WA4 4AD

Received January 24, 1996. Revised Manuscript Received March 12, 1996[⊗]

Real-time in situ energy-dispersive X-ray diffraction has been used to study the synthesis of the open-framework sulfide TMA−SnS-1, under hydrothermal conditions. The effects of varying the temperature of reaction, reactant source, and pH of solution on the synthesis have been studied. It is found that temperature is the primary factor in determining whether crystalline products are formed, while the pH of solution and reactant source were found to be important in determining the rate of reaction and the polytypic structure produced. Evidence has been obtained that in cases where crystalline TMA−SnS-1 is formed, the reaction proceeds via an intermediate disordered lamellar phase, before reacting further to form the final product.

Introduction

Hydrothermal synthesis has been extensively used for the production of microporous inorganic materials[1,2] consisting of three-dimensional networks of regularly sized and shaped voids and channels. These structural features give these materials a number of unique properties, such as selective absorption and catalysis,[3] and has led to their use as molecular sieves and ion-exchange reagents. Recently there has been much interest in using the precise pore structures of microporous materials to control the dimensions and properties of compounds constrained within their cavities.[4−6]

The vast majority of open framework materials synthesised to date have been oxides such as zeolites[2,7−10] and aluminophosphates,[11] which consist of frameworks built by linking together MO_4 units (M = Si, Al, P) to form a regular array of cavities and channels. However, in 1989 Bedard and co-workers reported the synthesis of a new class of metal sulfide based microporous materials denoted R−MS-*n* (where M = Sn or Ge, *n* represents different structural types, and R is an included organic molecule).[12,13] Since then, others have synthesized further compounds in this class and have incorporated different metallic elements into the frameworks.[14−20] The synthetic method employed is similar to the techniques used for the production of oxide microporous solids; the starting materials are heated under autogenous hydrothermal conditions in the presence of a templating agent. The templating agent (R) is typically an amine or quaternary ammonium salt. The use of different templates can lead to materials with a range of pore sizes.[21] These microporous sulfides represent a significant departure from oxide-based materials. As the original literature points out,[12,13] the presence of low-lying d orbitals and its greater size gives sulfur a far richer coordination chemistry than oxygen, and the greater rigidity of M−S−M linkages relative to M−O−M linkages should lead to the formation of more open structures with novel electronic and catalytic properties. In contrast to insulating oxide materials, these sulfides are semiconductors and a variety of possible applications can be envisaged for them.[21]

[⊗] Abstract published in *Advance ACS Abstracts,* July 15, 1996.

(1) Barrer, R. M. *Hydrothermal Chemistry of Zeolites*; Academic Press: London, 1982.
(2) Davis, M. E.; Lobo, R. F. *Chem. Mater.* **1992**, *4*, 756−768.
(3) Csicsery, S. M. *Chem. Br.* **1985**, *21*, 473−477.
(4) Herron, N.; Wang, Y.; Eddy, M. M.; Stucky, G. D.; Cox, D. E.; Moller, K.; Bein, T. *J. Am. Chem. Soc.* **1989**, *111*, 530.
(5) Ozin, G. A. *Adv. Mater.* **1992**, *4*, 612.
(6) Stucky, G. D.; Dougall, J. E. M. *Science* **1990**, *247*, 669.
(7) Breck, D. W. *Zeolite Molecule Sieves: Structure, Chemistry and Use*; Wiley and Sons: London, 1974.
(8) Szostak, R. *Molecular Sieves: Principles of Synthesis and Identification*; Van Nostrand Reinhold: New York, 1989.
(9) van Bekkum, H.; Flanigen, E. M.; Jansen, J. C. *Introduction to Zeolite Science and Practice*; Elsevier: Amsterdam, 1991.
(10) Barrer, R. M. *Zeolites and Clay Minerals as Sorbents and Molecular Sieves*; Academic Press: London, 1978.
(11) Bennett, J. M.; Dytrych, W. J.; Pluth, J. J.; Richardson, J. W.; Smith, J. V. *Zeolites* **1986**, *6*, 349.
(12) Bedard, R. L.; Vail, L. D.; Wilson, S. T.; Flanigen, E. M. U.S. Patent 4,880,761, 1989.
(13) Bedard, R. L.; Vail, L. D.; Wilson, S. T.; Flanigen, E. M. U.S. Patent 4,933,068, 1990.
(14) Parise, J. B.; Ko, Y.; Cahill, C. L. *J. Chem. Soc., Chem. Commun.* **1994**, 69.
(15) Parise, J. B.; Ko, Y. *Chem. Mater.* **1994**, *6*, 718−720.
(16) Parise, J. B.; Ko, Y.; Tan, K.; Nellis, D. M.; Koch, S. *J. Solid State Chem.* **1995**, *117*, 219−228.
(17) Kim, K. W.; Kanatzidis, M. G. *Inorg. Chem.* **1993**, *32*, 4161−4163.
(18) Chou, J.-H.; Kanatzidis, M. G. *Chem. Mater.* **1995**, *7*, 5−8.
(19) Parise, J. B. *Science* **1991**, *251*, 292.
(20) Parise, J. B.; Ko, Y. *Chem. Mater.* **1992**, *4*, 1446.
(21) Ahari, H.; Bowes, C. L.; Jiang, T.; Lough, A.; Ozin, G. A.; Bedard, R. L.; Petrov, S.; Young, D. *Adv. Mater.* **1995**, *7*, 375−378.

S0897-4756(96)00047-6 CCC: $12.00

Clearly these materials are of great technological and academic interest. However, in many cases the correct synthetic conditions to produce pure crystalline products are achieved only by a process of little more than "trial and error". A greater understanding of the crystal-growth process, the kinetics and mechanism of formation, the effect of changing reaction variables, and the role of the templating agent is needed if more rational syntheses of these materials are to be devised. Although some progress in understanding the formation processes has been gained from neutron diffraction[22] and X-ray scattering studies,[23] the precise details are still unknown.

In situ X-ray diffraction experiments provide a powerful method of obtaining information about these reactions, since they involve the direct observation of the formation of the crystalline product phase.[24] This offers a number of advantages over other techniques. First, it eliminates the need for quenching and workup, during which the sample may undergo significant and indeterminable structural changes. Second, it allows the direct observation of crystalline intermediate phases and their subsequent transformation into the product phase. Finally, in situ experiments provide an easy method for determining the effect of changing reaction variables and allow one to monitor the interconversion of different phases as conditions are varied. Over the past few years a number of in situ diffraction studies have been published.[22−32]

It is advantageous to use energy-dispersive diffraction techniques using "white" synchrotron radiation in this work, because the high intensity of such radiation can penetrate the thick-walled high-pressure reaction cells needed for this work, without serious loss of intensity. This allows high-quality spectra to be collected quickly, permitting time-resolved studies to be undertaken.

In this paper we describe the use of time-resolved in situ diffraction experiments to study the formation of the microporous tin sulfide TMA−SnS-1 under isothermal hydrothermal conditions, using a specially constructed apparatus, the design of which is also outlined. A similar study of the crystallization of CoALPO-5 using the hydrothermal cell descibed herein has recently been undertaken by Thomas and co-workers.[33,34]

Experimental Section

Synthesis. TMA−SnS-*n* phases were synthesized in a manner similar to those described previously.[12,13,35,36] Reaction compositions of either 1Sn:2.2S:1TMAOH:nH$_2$O where n = 15−100, or 3SnS$_2$:2S:2TMAOH:nH$_2$O where n = 30−65, were reacted under isothermal hydrothermal conditions (TMAOH = tetramethylammonium hydroxide). Tin (or tin disulfide) and sulfur were added to solutions of tetramethylammonium hydroxide with stirring. The tin disulfide used had been previously synthesized by reaction of stoichiometric quantities of the elements in sealed, evacuated silica ampules at 560 °C for 1 week, as described by Al-Alamy and Balchin,[37] and was then ground and sieved to a particle size of <90 μm before reaction. Collection of data was started as quickly as possible after mixing of the reagents. The delay between mixing and the start of data collection was less than 1 min, which is insignificant compared to the time scale of the reaction. The reaction mixtures were stirred throughout. Precise reaction conditions and stoichiometries for each experiment are detailed later at the appropriate points.

Diffraction Experiments. Time-resolved X-ray diffraction experiments were performed on stations 9.7 and 16.4 of the UK Synchrotron Radiation Source at Daresbury Laboratory. Reactions were performed either in sealed thick-walled (3 mm) glass ampules or in a hydrothermal pressure cell we had previously designed for studying hydrothermal reactions using energy-dispersive radiation.[38] Technical details of the station design and experimental technique have been described by ourselves and others elsewhere,[39−42] and only a brief description will be given here. Stations 9.7 and 16.4 receive X-ray flux in the range 5−140 keV, with a maximum intensity at about 20 keV. The position of the maximum intensity at the detector is, however, shifted to higher energy on introduction of the experimental apparatus, due to the absorption of lower energy photons by the cell materials. Useful intensity could be obtained above about 20 keV using the glass ampules, or above 40 keV using the cell. Since the energy, E (keV), at which a Bragg reflection from planes of separation d (Å) is given by $E = 6.19926/d \sin\theta$, a detector angle (2θ) of between 1.6° and 2.2° was chosen for all experiments, giving an observable d-spacing range of 4−13 Å. As the highest d-spacing peak of interest occurs at 11.5 Å, this is an ideal angle for the study of these syntheses.

In all experiments, resonances, which arise due to excitation of core electrons of the elements present by X-rays, were seen. The most intense of these were the Sn Kα and Kβ resonances at 25.2 and 28.4 keV. These proved useful, because by normalizing against the intensity of these resonances, it is possible to correct for changes in intensity of Bragg reflections due to factors such as decay of the synchrotron beam current with time.

The station electronics and data collection software were configured so that a series of spectra could be recorded during the course of a reaction. Acquisition times of 120−300 s were chosen as this was a short enough period for kinetic and structural studies to be performed, while still giving good counting statistics.

Design of the Hydrothermal Cell. A detailed technical report on the design and commissioning of the hydrothermal

(22) Iton, L. E.; Trouw, F.; Brun, T. O.; Epperson, J. E. *Langmuir* **1992**, *8*, 1045−1048.
(23) Dokter, W. H.; Beelen, T. P. M.; Garderen, H. F. v.; Santen, R. A. v.; Bras, W.; Derbyshire, G. E.; Mant, G. R. *J. Appl. Crystallogr.* **1994**, *27*, 901.
(24) Munn, J.; Barnes, P.; Häusermann, D.; Axon, S. A.; Klinowski, J. *J. Phase Trans.* **1992**, *39*, 129.
(25) Clausen, B. S.; Grabaek, K.; Steffensen, G.; Hansen, P. L.; Topsoe, H. *Catal. Lett.* **1993**, *20*, 23.
(26) Norby, P.; Christensen, A. N.; Hanson, J. C. *Stud. Surf. Sci. Catal.* **1994**, *84*, 179.
(27) Christensen, A. N.; Norby, P.; Hanson, J. C. *J. Solid State Chem.* **1995**, *114*, 556.
(28) Sankar, G.; Thomas, J. M.; Wright, P. A.; Natarajan, S.; Dent, A. J.; Dobson, B. R.; Ramsdale, C. A.; Greaves, G. N.; Jones, R. H. *J. Phys. Chem.* **1993**, *97*, 9550.
(29) Thomas, J. M.; Greaves, G. N. *Science* **1994**, *265*, 1675.
(30) Sankar, G.; Rey, F.; Thomas, J. M.; Greaves, G. N.; Corma, A.; Dobson, B. R.; Dent, A. J. *J. Chem. Soc., Chem. Commun.* **1994**, 2279.
(31) Sankar, G.; Thomas, J. M.; Rey, F.; Greaves, G. N. *J. Chem. Soc., Chem. Commun.* **1995**, 2549.
(32) Thomas, J. M.; Greaves, G. N.; Sankar, G.; Wright, P. A.; Chen, J. S.; Dent, A. J.; Marchese, L. *Angew. Chem., Int. Ed. Engl.* **1994**, *33*, 1871.
(33) Rey, F.; Sankar, G.; Thomas, J. M.; Barrett, P. A.; Lewis, D. W.; Catlow, C. R. A.; Clark, S. M.; Greaves, G. N. *Chem. Mater.* **1995**, *7*, 1435.
(34) Rey, F.; Sankar, G.; Thomas, J. M.; Barrett, P. A.; Lewis, D. W.; Catlow, C. R. A.; Clark, S. M.; Greaves, G. N. *Chem. Mater.* **1996**, *8*, 590 (Corrigendum).
(35) Parise, J. B.; Ko, Y.; Rijssenbeek, J.; Nellis, D. M.; Tan, K.; Kock, S. *J. Chem. Soc., Chem. Commun.* **1994**, 527.
(36) Ahari, H.; Ozin, G. A.; Bedard, R. L.; Petrov, S.; Young, D. *Adv. Mater.* **1995**, *7*, 370−374.
(37) Al-Alamy, F. A. S.; Balchin, A. A. *J. Cryst. Growth* **1977**, *38*, 221.
(38) Evans, J. S. O.; Francis, R. J.; O'Hare, D.; Price, S. J.; Clarke, S. M.; Flaherty, J.; Gordon, J.; Nield, A.; Tang, C. C. *Rev. Sci. Instrum.* **1995**, *66*, 2442−2445.
(39) Clark, S. M. *Nucl. Instrum. Methods A* **1989**, *276*, 381.
(40) Clark, S. M.; Miller, M. C. *Rev. Sci. Instrum.* **1990**, *61*, 2253.
(41) Clark, S. M. *Rev. Sci. Instrum.* **1992**, *63*, 1010.
(42) Clark, S. M.; Irvin, P.; Flaherty, J.; Rathbone, T.; Wong, H. V.; Evans, J. S. O.; O'Hare, D. *Rev. Sci. Instrum.* **1994**, *65*, 2210.

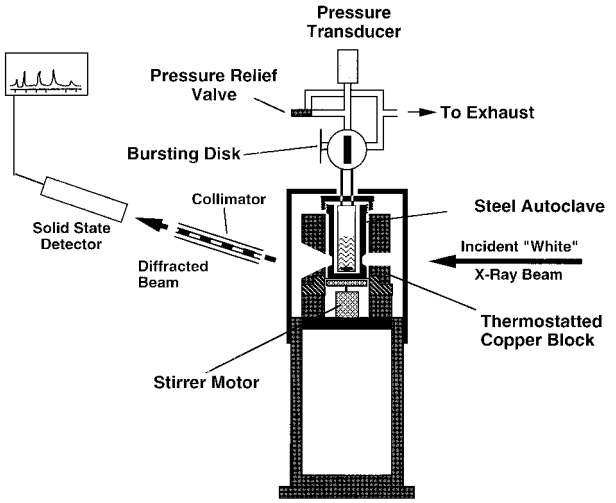

Figure 1. Schematic diagram of the experimental apparatus used for in situ diffraction studies of hydrothermal reactions. Also shown is the hydrothermal pressure cell; in some lower pressure reactions this was replaced by thick-walled glass ampules.

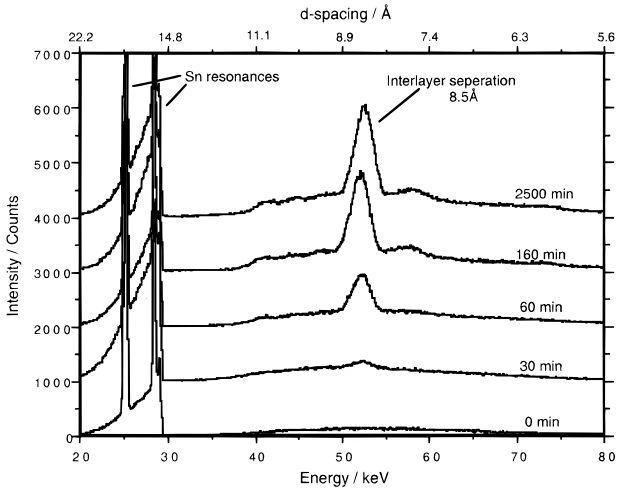

Figure 2. Stack plot showing the time evolution of the diffraction pattern of the reaction of 1Sn:2.2S:1TMAOH:35H_2O at 120 °C. Acquisition time for each spectra was 300 s. Spectra were recorded at a 2θ angle of 1.6°. Individual spectra have been normalized using the Sn Kα resonance at 25.2 keV.

cell and the sample control enviroment has been published elsewhere.[38] However, a brief description is given here. (See also Figure 1.) The cell design takes advantage of commercially available connectors, heads, and pressure gauge assemblies. A stainless steel tube, closed at one end, of external diameter 29.7 mm, internal diameter 25.4 mm, and height 93 mm was machined from a piece of solid stainless steel. The cell wall thickness was then machined down to 0.7 mm over a 29 mm height range through which the incident and diffracted beam pass. This window allows a large enough flux of X-rays to pass through the cell to permit time-resolved studies to be carried out. Because of the corrosive reagents used in hydrothermal syntheses, a Teflon liner and lid were manufactured to fit inside the cup to minimize the contact between reagents and the cell walls. The cell body was connected to a standard Parr Instruments head and gauge block assembly fitted with a pressure relief valve and rupture disk. The rupture disk has a recommended maximum working pressure was 700 psig (~50 bar). For safety reasons a maximum working pressure of 400 psig (~29 bar) was chosen.

Sample Control Environment. Sample heating was achieved by circulating hot oil through a solid copper block using a Fisons Haake S oil circulator. Gantries were cut through the block to allow the passage of hot circulating oil and a 30 mm hole was cut into which the ampules or cell fitted snugly. The maximum sample temperature attainable was found to be 227 °C. Slots were cut into the side of the block for both the incident and exit beam. Threads were tapped into the top of the block for attachment of thermocouples. The block was then mounted on a stand containing a magnetic stirring device to allow sample stirring during reaction. Tests indicated that block temperatures were stable to ±1 °C, and the temperature of the sample was within 1 °C of the block temperature. The thermal lag between the block and liquid within the ampules or cell was less than 2 min. A diagram of the experimental apparatus is shown in Figure 1.

Results and Discussion

TMA−SnS-1 (empirical formula $(NMe_4)_2Sn_3S_7 \cdot xH_2O$, $x = 1-3$) is synthesized by reaction of a tin and sulfur source under basic hydrothermal conditions in the presence of TMA^+ cations (TMA = tetramethylammonium). The chemistry of this system is known to be complex. At least two structural forms of TMA−SnS-1 are known. One is a monoclinic form whose structure was determined by single-crystal XRD,[35] the other is an orthorhombic modification, which is assumed to be isostructural with its selenium analogue, whose structure has been determined by single-crystal XRD.[21,36] Both of these forms contain the same basic structural units; stacks of $Sn_3S_7^{2-}$ layers with charge-balancing TMA^+ cations between the layers. Individual layers consist of 24 atom-ring hexagonal pores built from interconnected Sn_3S_4 clusters which create an open-framework structure. The orthorhombic form shows a slight structural deformation of the pores relative to the monoclinic form and has a different layer-stacking sequence. The structural complexity and the strong dependence of the reaction product on the precise reaction conditions used made this an interesting system to study. We report here the results of an investigation of the synthesis of TMA−SnS-1 by in situ energy-dispersive X-ray diffraction using a variety of different reaction temperatures, source materials, and starting pH.

Variable-Temperature Measurements. To investigate the effect of the variation of temperature on the formation of TMA−SnS-1, mixtures of constant composition 1Sn:2.2S:1TMAOH:35H_2O were reacted under hydrothermal conditions at the representative temperatures of 120, 150, and 175 °C in thick-walled glass ampules.

The behavior of the reactions at 120 and 150 °C was similar. After an induction period of approximately 20 min a broad peak at 8.5 Å became visible and grew rapidly in intensity over the next 120 min and then at a much slower rate for the next 3 days. However, even after prolonged heating only a few other very broad and weak peaks could be seen in the diffraction pattern. Figure 2 shows a stack plot of the evolution with time of the energy-dispersive diffraction pattern for the reaction performed at 120 °C. Note the long time interval between the last two spectra with no noticeable change in the diffraction pattern.

Laboratory X-ray diffraction patterns of the worked up samples also showed only broad and weak peaks except for the reflection at 8.5 Å. However, peaks assignable to both monoclinic and orthorhombic polytypes could be seen. Since a *d* spacing of 8.5 Å corresponds to the interlayer separation in TMA−SnS-

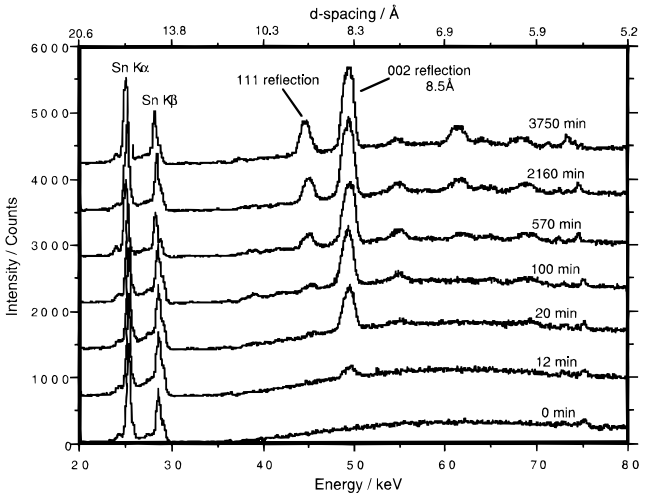

Figure 3. Stack plot showing the time evolution of the diffraction pattern of the reaction of 1Sn:2.2S:1TMAOH:35H_2O at 175 °C. Acquisition time for each spectra was 120 s. Spectra were recorded at a 2θ angle of 1.72°. Individual spectra have been normalized using the Sn Kα resonance.

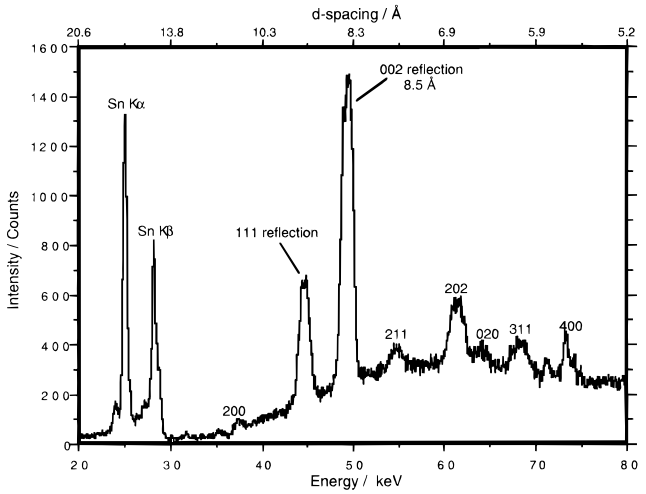

Figure 4. Spectrum of the final product from the reaction of 1Sn:2.2S:1TMAOH:35H_2O at 175 °C. Acquisition time was 120 s at a 2θ angle of 1.72°. The spectrum is indexed on the orthorhombic cell a = 22.9, b = 13.1, c = 16.7 Å.

1, it appears that under the above conditions a layered material is formed rapidly which is ordered in the direction perpendicular to the layers but is highly disordered in the plane of the layers, and a fully three-dimensionally ordered structure is not formed even after prolonged heating.

When the same reaction was performed at 175 °C a different type of behavior was seen. Figure 3 shows a stack plot of the time evolution of the diffraction pattern for this reaction. As in the previous reactions, after a short induction period of approximately 10 min, a Bragg peak centered at 8.5 Å became visible and grew rapidly in intensity, but in this case other peaks became visible after approximately 15 min and gradually grew in intensity. After 3 days of heating, the diffraction pattern was essentially constant with time and many strong diffraction peaks could be seen. Figure 4 shows the final observed pattern.

All of the peaks in Figure 4 can be indexed as peaks in the diffraction pattern of orthorhombic TMA−SnS-1, and only a very small quantity of monoclinic impurity was formed. No intermediate crystalline phases were

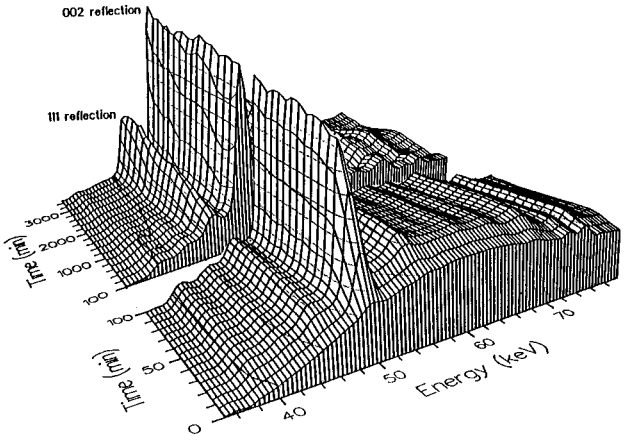

Figure 5. Three-dimensional plot showing the time evolution of the diffraction pattern of the reaction of 1Sn:2.2S:1TMAOH:35H_2O at 175 °C, showing the initial rapid growth of the 002 reflection, followed by the much slower growth of the 111 reflection. Note the change in scale of the time axis at 100 min.

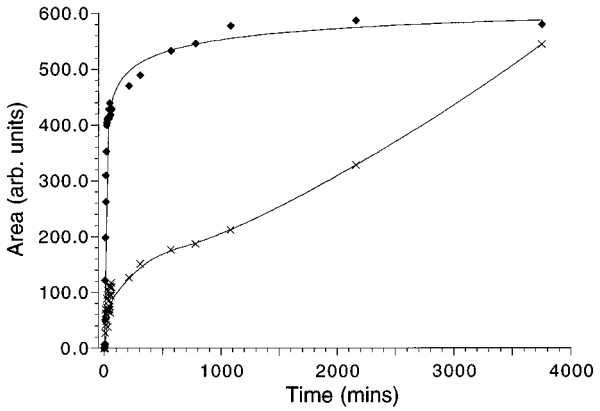

Figure 6. Plot of peak area against time for the 002 (♦) and 111 (×) reflections of orthorhombic TMA−SnS-1 during the reaction of 1Sn:2.2S:1TMAOH:35H_2O at 175 °C. Intensities have been normalized using the Sn Kα resonance and scaled such that the final intensities are approximately equal. Lines are mathmatical fits only and have no physical significance.

observed, and these data show that under these conditions the orthorhombic form of TMA−SnS-1 crystallizes smoothly from the reaction mixture.

Kinetic analysis of the growth of the diffraction peaks was performed by integrating the peak intensities using a Gaussian fitting routine.[43] This analysis shows that each Bragg reflection does not obey the same rate law. Rather, the 002 peak at 8.5 Å (interlayer separation) grows very rapidly in the initial stages of the reaction, followed by a longer period of much slower growth, while other *hk*0 and *hkl* reflections show an initial rapid growth followed by a period of steady growth. Figure 5 shows a three-dimensional plot of the evolution of the diffraction peaks with time and shows the increase in relative intensity of the *hk*0 and *hkl* reflections, especially the 111 reflection, during the course of the reaction.

Figure 6 shows a comparison of the growth with time of the 002 and 111 reflections. The intensities have been normalized using the Sn Kα resonance, and scaled such that the final intensities are similar. (In reality the 002 reflection is always more intense than the 111

(43) Clark, S. M. *J. Appl. Crystallogr.* **1995**, *28*, 646−649.

reflection.) It can be seen that the growth of the 002 peak is essentially complete after just 200 min of reaction, whereas the 111 reflection is still growing strongly at a much later stage. (In fact the data suggest that the 111 reflection was still growing in intensity, indicating that the reaction had not proceeded fully to completion.) Similar behavior is seen for other non 00*l* reflections, although the increase in relative intensity is most marked for the 111 reflection.

The rate of growth of the 002 reflection gives an indication of how quickly layers stack together, while the rate of growth of the 111 reflection gives an indication of how quickly layers order with respect to adjacent layers. Therefore these data are strongly suggestive of a two-stage process, whereby in the initial stages a layered but fairly disordered material is rapidly formed, followed by a much slower process in which this material orders in three dimensions to give the final observed phase. More discussion of this process follows later.

Other reactions (using the same reactant stoichiometry) were performed at higher temperatures and pressures in a hydrothermal pressure cell. At temperatures between 175 and 200 °C no significant changes in the reaction pathway were observed. However, as the temperature was raised above 200 °C (and autogenous pressures rose above 15 bar), there was evidence for a partial collapse of the structure to form tin disulfide. It is to be expected that as the reaction pressure increases, open-framework structures should become unstable and more condensed phases form (density of TMA−SnS-1 is ca. 2 g cm^{-1}, density of SnS_2 is ca. 4.5 g cm^{-1}). Unfortunately, beam time constraints meant that full investigation of this high-temperature process has not been possible, and we plan further experiments to study this more fully.

Variable-pH Measurements. To study the effect of pH on the reaction, mixtures with differing water-to-tin ratios but constant hydroxide to tin ratios were reacted at the constant temperature of 175 °C. The stoichiometries used were 1Sn:2.2S:1TMAOH:$n$$H_2O$ where n = 15, 30, 50, 75, and 100, which corresponds to pH's of 14.6, 14.3, 14.0, 13.9, and 13.7.

In general, all reactions followed a pathway similar to the reaction discussed above, i.e., the rapid growth of a Bragg peak corresponding to the interlayer separation, followed by the slower growth of other diffraction peaks. The most obvious difference between the reactions was the reaction rate. This was especially evident in the growth of the 8.5 Å interlayer peak during the initial stages of the reaction. Using a water stoichiometry of n = 15, the induction period is very short (~4 min) and the growth is very rapid; the intensity of the 8.5 Å peak reaches the "plateau" in approximately 15 min. At lower pH (i.e., higher water stoichiometries), both the induction period and the amount of time for the intensity to "plateau" progressively increase. Figure 7 shows a plot of the variation with time of the intensity of the 8.5 Å peak for the five reactions, normalized with respect to the tin Kα resonance, and with the intensity scales adjusted so that the intensity of the reflections at the plateau are all approximately the same.

The primary role of the OH^- ions in hydrothermal syntheses is thought to be the dissolution and complexation of the solid reagents (tin and sulfur in this case) to produce solution-phase ions. These complexes are transported through solution and then condense, presumably under the charge balancing, space filling, and structure-directing influence of the template, into the building blocks of TMA−SnS-1, which then crystallizes from solution. Ozin and co-workers have suggested the dimeric species $Sn_2S_6^{4-}$ as one possible intermediate in the formation of these materials.[44]

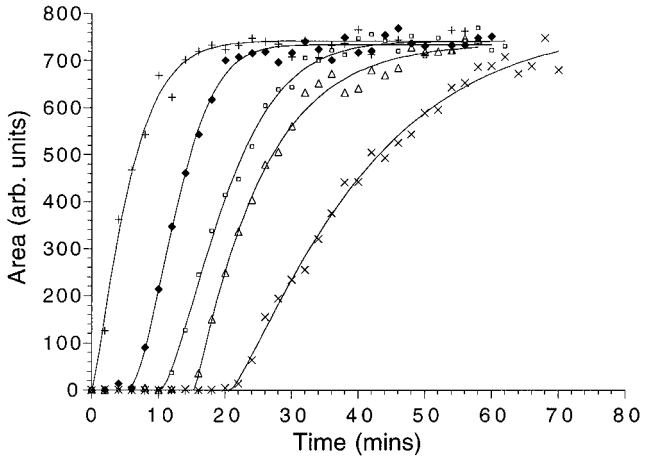

Figure 7. Plot of peak area against time for the 002 reflection of orthorhombic TMA−SnS-1 during the reaction of 1Sn:2.2S:1TMAOH:$n$$H_2O$ at 175 °C, for n = 15 (+), n = 30 (♦), n = 50, (O), n = 75 (△), and n = 100 (×). Intensities have been normalized using the Sn Kα resonance and scaled such that the final intensities are approximately equal. Lines are mathmatical fits only and have no physical significance.

These data, showing a faster rate of reaction and shorter induction time at high pH, are consistent with this role. It would be expected that a greater concentration of hydroxide ions would lead to a greater rate of dissolution of the solid reagents, which is likely to be the primary factor in determining the induction period. [An unavoidable additional factor in these experiments is the time it takes for the reagents to heat from room temperature to the reaction temperature. Past experience with the experimental apparatus suggests this time period is short, less than 2 min. Although, clearly, this is a significant fraction of the induction period, especially in the high-pH reactions, this time factor will be very similar for all reactions, so this effect should not cause the differences seen in induction times for the reactions.]

The rate of growth of the crystalline phase is presumably related to the rate at which solubilized species diffuse together and condense, which will be related to their concentration in solution. Again, a higher initial concentration of hydroxide ions would be expected to yield a greater concentration of solubilized tin/sulfur species and hence a faster rate of growth.

In all cases the predominant product was orthorhombic TMA−SnS-1. However, subtle differences in the precise product formed were observed. At high pH (n = 15 and 30) a virtually pure orthorhombic phase was formed, but the reaction where n = 50 gave a mixed reaction product, mostly orthorhombic but with a significant monoclinic impurity. As the pH was lowered progressively (n = 75, 100) the quantity of monoclinic polytype relative to the orthorhombic polytype increased

(44) Ozin, G. A.; Jiang, T.; Bedard, R. L. *Adv. Mater.* **1994**, *6*, 860−865.

steadily. It is not clear why a reduction in pH of solution should lead to such an effect. It is possible that the ratio of water to tin, which is also being varied here, is another important factor in these experiments. We plan further experiments in which the quantity of water and TMA^+ is kept constant, but the pH is adjusted using HCl, to gain insight into the relative importance of the various factors. We also plan to study a wider pH range.

Effect of Reactant Source. To study the effect of the tin and sulfur starting materials on the reaction, an experiment was performed in which the elemental tin and sulfur were replaced by a mixture of tin disulfide and sulfur. A composition $3SnS_2$:2S:2TMAOH:$60H_2O$ was reacted at 175 °C.

Three noticeable changes were seen. These were to the reaction rate, reaction product, and reaction crystallinity. The reaction rate was found to be much slower using tin disulfide than in the corresponding reaction using elemental tin and sulfur as the source materials. There was an induction period of 30 min before the first diffraction peak, at 8.5 Å, was seen (as opposed to <10 min in the analogous tin/sulfur case), and the growth of the diffraction peaks was very slow. Even after 3 days of reaction, diffraction peaks due to the product were fairly weak and a significant quantity of tin disulfide starting material was left unreacted.

Again, this can be rationalized in terms of the role of the hydroxide ion; specifically, the resistance of tin disulfide to dissolution by hydroxide ions relative to tin and sulfur, which are well-known to readily form hydroxide complexes in solution. This leads to a low rate of dissolution and hence a slow rate of formation of product.

In general the reaction gave a less pure and less crystalline product than the corresponding reaction using elemental tin and sulfur as the starting materials. Only broad and fairly weak peaks were seen in the diffraction pattern. Laboratory XRD of the worked-up sample confirmed that the product was poorly crystalline and, although mostly the monoclinic polytype, contained significant quantities of the orthorhombic polytype and other minor phases. This observation may seem at odds with the fact that the original literature used tin disulfide as starting materials,[12,13] and Parise and co-workers have obtained pure crystalline phases using tin disulfide.[16,35] However, the conditions used were not precisely the same as in this experiment. In particular the use of crystalline as opposed to amorphous tin disulfide is likely to be an important factor. The observation is simply that under *this particular* set of conditions, less crystalline samples are produced using tin disulfide as a starting material.

As in the case of the variable pH reactions, the reasons for changes in product composition as conditions are varied are not easy to rationalize. Clearly more work is required to fully understand these systems. However, it appears that the monoclinic form is formed preferentially in the slower reactions (i.e., those carried out at lower pH, or using tin disulfide as a starting material), when the concentration of dissolved species in solution is lower. This may indicate that the monoclinic form is the thermodynamically more stable form and that when the reaction is slow enough the true stable product is formed, i.e., monclinic TMA−SnS-1. This is consistant with the results of Ozin and co-workers on the analogous selenium compound TMA−SnSe-1.[21] It was found that early stages of the synthesis orthorhombic TMA−SnSe-1 was formed, but at later times the monoclinic form was obtained, suggesting that the monoclinic form is the thermodynamic product of that system.

Discussion of Mechanism

The results detailed in the above sections, together with results from other in situ experiments, can be collated to give an overall picture of the mechanism of formation of TMA−SnS-1 materials. These studies suggest that the formation of these materials occurs via a three-stage mechanistic pathway.

The first stage is the dissolution and complexation of the solid reagents by the OH^- mineralizing agent, followed by their condensation into the tin polysulfide units that provide the building blocks for the formation of the SnS-1 structure. These processes occur during the "induction" period of the reaction, and this stage is found to occur very quickly, with a rate that is dependent on the OH^- concentration.

The second stage is the rapid (on a time scale of minutes to hours) growth of a poorly crystalline layered material. This material is ordered in the direction perpendicular to the tin sulfide layers (as indicated by the strong reflection corresponding to the interlayer separation) but highly disordered in the plane of the layers (as indicated by the absence of any other strong reflections). It is presumably during this stage that the template plays a crucial structure directing role, providing charge balance for the growing tin sulfide layer and filling space between the layers.

The third stage is a solid-state reorganization to form a crystalline material which is ordered in three dimensions with a regular stacking arrangement, i.e., it is the formation of a distinct polytype from a disordered layer arrangement. This process is indicated by the growth of many strong peaks in the diffraction pattern. This stage of the mechanism is much slower, taking place on a time scale of days. A schematic diagram of this proposed mechanism is shown in Figure 8.

It is found that regardless of the synthetic conditions applied, in all cases studied the reaction proceeded through the first two stages of the mechanism, indicating that the formation of tin sulfide layers is a ubiquitous phenomenon in this system. However, the third stage of the process was not observed in all cases but only under certain very specific conditions of temperature, reactant source, and reaction composition. Temperature was found to be the most important factor in determining the crystallinity of the final product.

It is to be expected that the thermodynamically most favored state is the one in which the tin sulfide layers are ordered with respect to each other, with the TMA^+ cations "locked into" the host lattice, because this would lead to an enhanced lattice energy. Therefore the two latter stages of reaction could be considered to be the initial formation of the kinetic product (the disordered layer structure), followed by a gradual transformation into the thermodynamic product (an ordered polytype). The fact that temperature is such an important factor in determining if the third stage of the process occurs may mean that there is a large activation barrier associated with the layer shifts needed for the rear-

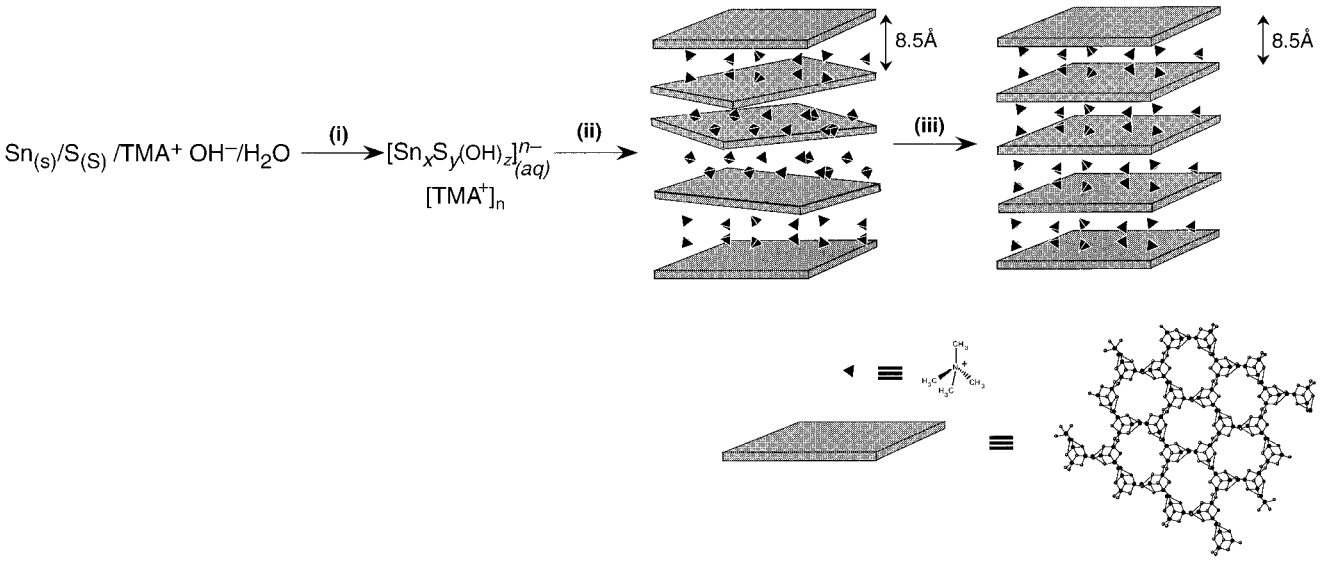

Figure 8. Schematic representation of the proposed mechanism of formation of TMA−SnS-1. (i) Dissolution of the solid reagents by OH^- ions to form solution-phase ions. (ii) Condensation of these ions under the influence of the template to form a disordered layered material. (iii) Solid-state reorganization to form a fully three-dimensionally ordered structure. Stage ii is rapid (on a time scale of minutes to hours), and occurs under all conditions studied, whereas stage iii is slow (on a time scale of days) and occurs only under certain reaction conditions, primarily a high enough temperature.

rangement from a disordered to ordered layer structure and that a sufficiently high temperature is needed for this to occur at an observable rate. Alternatively, the rearrangement may occur via a process of continuous formation and redissolution of the product phase, which occurs only under fairly vigorous conditions of temperature and pH. In other cases the kinetic product cannot be redissolved and hence is the final product of the system.

Conclusion/Summary

This paper has described the use of real-time in situ energy-dispersive X-ray diffraction experiments to study the formation of the open-framework sulfide TMA−SnS-1. A mechanistic model has been proposed in which under certain synthetic conditions, primarily a high enough temperature, the final crystalline product is formed via an intermediate disordered lamellar phase. Under other conditions, this disordered phase is found to be the final observed product. The rate of formation of the layered material is found to be strongly dependent on the reaction temperature, pH of solution, and source material used. In those cases where a well-defined crystalline product is formed, which polytype is formed, or, in the case of mixtures, the relative quantities of each, is found to be very sensitive to reaction variables such as the source materials or pH of solution. We are currently performing experiments to further probe the relationship between the reaction variables and the polytype formed and to determine under what conditions interconversion from one polytype to another can be achieved.

Although in this paper we have not reported any detailed kinetic analysis of the crystal-growth process, the data are of sufficiently high quality that such analysis is feasible. We believe that this in situ study has shown that useful information about the kinetics and mechanism of hydrothermal syntheses can be obtained using this technique. We feel that it has wide application for the study of the formation of a variety of microporous materials synthesised under hydrothermal conditions, such as zeolites, aluminophosphates, chalcogenides, and metal phosphates.

Acknowledgment. We would like to thank DRAL for a CASE studentship (R.J.F.) and the use of the Synchrotron Radiation Source facility, and Daresbury Laboratory technical staff for helping in the design and constuction of the experimental apparatus and hydrothermal cell.

CM960047C